

A Proposal for a Practical Heavy Mars Lander

October 15, 2008

I – Introduction

MarsDrive is an international organization dedicated to the exploration and settlement of space. Our Vision is of humanity becoming a space faring civilization. Our Mission is to enable and in every way support the rapid expansion of humanity into space by providing funds to research and develop the infrastructure necessary to establish a sustainable space economy which includes settlements and research facilities in places like the Moon and Mars.

Technologies exist today for travelling 99% of the distance between the Earth and Mars. We know how to get large payloads from the surface of the Earth to orbit around Mars. On the return trip, we know how to get from the surface of Mars all the way back to Earth. The problem is that last hundred miles from Mars orbit to the surface.

To that end, this proposal outlines the concept for a practical lander of 50 metric tons mass at Mars Entry Interface. This is sufficient to land a crew of five or six while not exceeding either the mass-to-LEO (low-earth orbit) or the shroud diameter of expected near-term launch vehicles already being designed by sources other than NASA. Further, this concept relies primarily on proven state-of-the-art technologies. It does not require any major technological breakthroughs such as lifting bodies which imply long-lead-time and very expensive developmental efforts. All technologies are either in use today or are relatively modest engineering outgrowths of existing technologies.

II – Landing on Mars

The problem is that Mars has too much atmosphere. Powered Entry, Descent, and Landing (EDL) techniques proven during the Apollo lunar landings are not applicable to Mars. First, a power-only landing would require carrying extensive propellants from Earth, immediately doubling the Initial Mass in Low-Earth Orbit (IMLEO) of the mission. Second, firing the descent propulsion engines into a high-hypersonic windstream during the early and mid-phases of the EDL is not possible. For much of the entry phase the windstream velocity exceeds the exhaust velocity of modern chemical propellant engines.

The problem is that Mars does not have enough atmosphere. Ballistic EDL techniques which have been well-proven on Earth since the days of Project Mercury simply do not work on Mars. The Martian atmosphere is too thin to slow an entry vehicle of realistic size to subsonic speeds. Hypersonic parachutes capable of slowing a 50 metric ton lander to low-subsonic speeds would be well over 100 meters in diameter and are presently well beyond state-of-the-art design[1]. Such an entry vehicle would still require a robust descent propulsion system to achieve the pinpoint landing necessary to rendezvous with pre-positioned assets at the designated landing site.

Clearly, some sort of hybrid system which combines the advantages of Ballistic and Powered EDL and which avoids, or at least minimizes, their respective disadvantages promises the optimal solution. A ballistic entry vehicle transitioning to a powered landing offers the best combination of the two. What remains is to optimize the transition point and to solve two particularly vexing transition problems.

Our investigation centered on an Apollo-legacy heatshield-plus-truncated-cone profile. This geometry is well-understood and has proven itself to be a near-optimal design. After abandoning this configuration in favor of the winged Space Transportation System geometry in the 1970s, NASA has finally returned to the proven Apollo entry geometry as evidenced by their decisions in the Orion / Constellation program [2]. As will be shown, a 14.5-meter diameter heatshield leading a 30° conic entry vehicle can decelerate a 50 metric ton vehicle to below Mach 2 at an altitude above 0 km based on the Mars Orbital Laser Altimeter (MOLA) survey.

The terminal deceleration to hover, cross-range maneuvering to the precise desired landing site, and the landing maneuver is accomplished by a liquid-fueled throttleable propulsion system. For the purposes of this study a liquid-oxygen / liquid-methane system was assumed for maximum compatibility with known *in situ* resources.

As previously stated, two major problems exist in the transition from ballistic flight to powered flight. At approximately Mach 1.5 the engines must be uncovered, ignited, and exposed to the windstream which is still supersonic. At the same time the heatshield must be discarded in such a way that it cannot come in contact with the lander. Unmentioned is the fact that a 14.5-meter heatshield is far larger than the maximum fairing diameter of any proposed launch vehicle.

III – The MarsDrive Common Lander

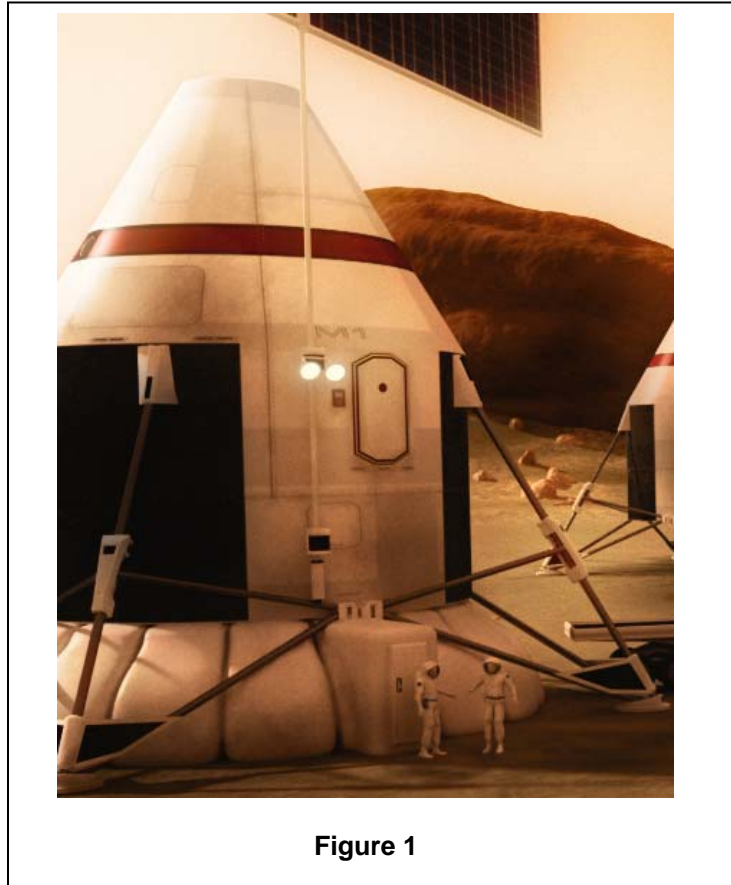
The MarsDrive Common Lander attempts to address these problems. As the name implies, the basic lander geometry is common to both crewed and uncrewed (cargo) landers used in a prototypical Mars exploration program. This commonality of design greatly reduces the development and certification cost of the mission hardware. It also provides a means of testing the concept at Mars without either flying a test mission with little or no useable delivered payload or flying a crew in an untested vehicle. Flying the Common Lander in its cargo configuration to deliver exploration rovers and, in a second flight, to deliver the crew's surface habitat to the designated landing site prior to the crewed mission, provides the opportunity to validate the vehicle's entry, descent, and landing (EDL) characteristics at Mars without placing a crew at risk in an untried vehicle. It also cuts the project's total development cost by requiring the design, development, and certification of only one EDL vehicle.

The Common Lander uses an Apollo-legacy heatshield-plus-truncated-cone profile. The vehicle enters the Martian atmosphere ballistically and is slowed by aerobraking. As the vehicle approaches Mach 1, the heatshield is discarded and the vehicle maneuvers to a landing propulsively. The use of supersonic parachutes to slow the vehicle between the aerobraking phase and the propulsive phase was considered, but was eventually discarded. Investigations by Braun and others [3] have shown that the advantages of an intermediate parachute stage diminishes as the entry mass increases, vanishing altogether around 60 metric tons of entry mass.

At the entry mass of the Common Lander, the small advantages of adding a parachute stage are offset by the increased risk of adding yet another element to what is already the riskiest part of the entire mission. Should further investigations reveal a significant advantage to adding a parachute stage in the transition from ballistic to powered flight, this option can be revisited with little or no affect on the overall mass budget.

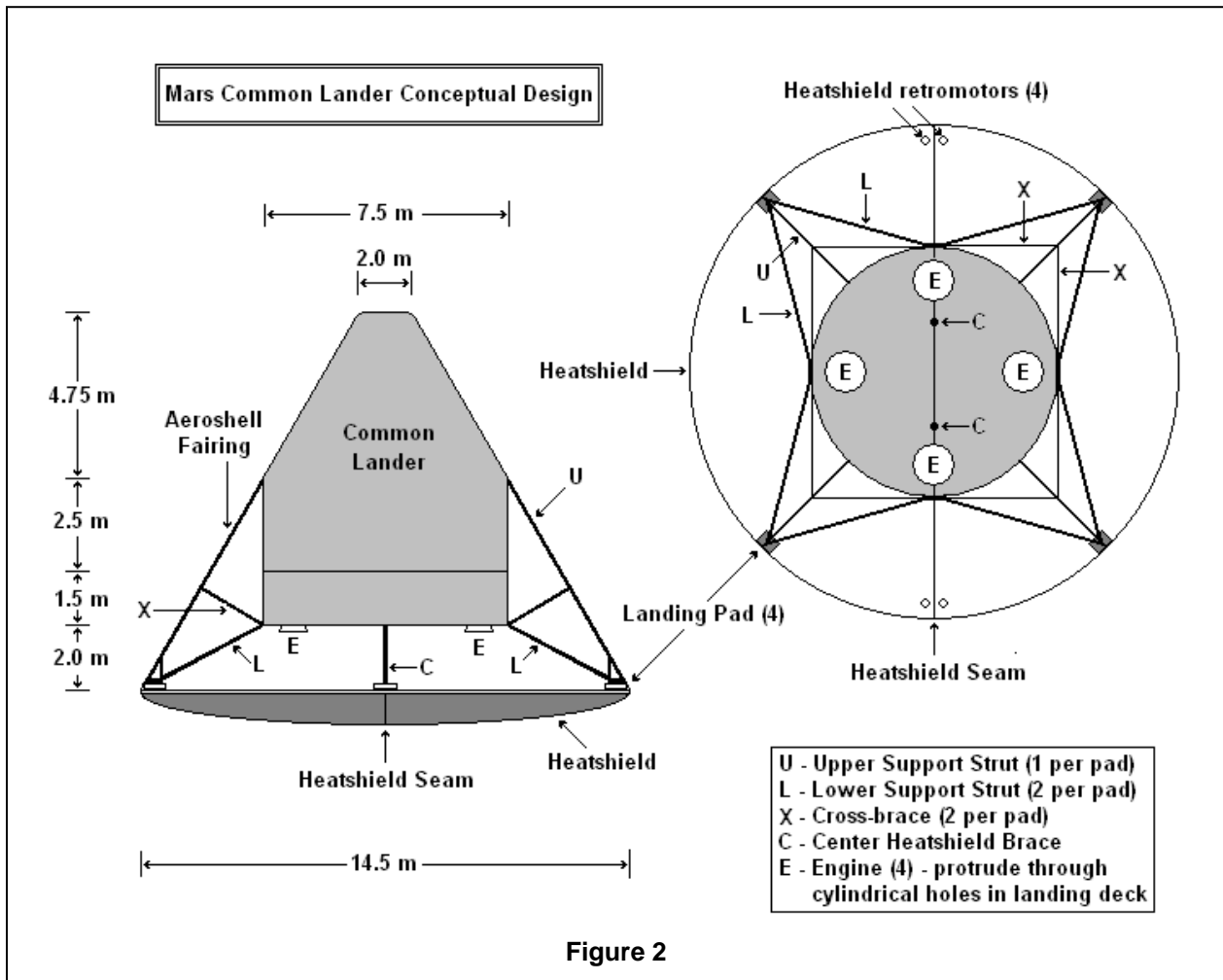
A self-imposed design constraint is that the Common Lander must fit within a 7.5-meter diameter launch vehicle payload fairing. However, this presents three significant problems. First, a 7.5-meter diameter heatshield proved to be insufficient to aerobrake the lander to the vicinity of Mach 1 during descent. Second, in order to ignite the landing engines, the heatshield, which covers the engines, must be discarded. Given the relative ballistic properties of the heatshield and the lander, it is difficult to see how this can be accomplished without the addition of a supersonic parachute. And third, igniting the landing engines while facing into a supersonic airstream is problematic.

The MarsDrive Common Lander is shown in Figure 1 as it might appear after landing on the Martian surface (Jason Archer design).



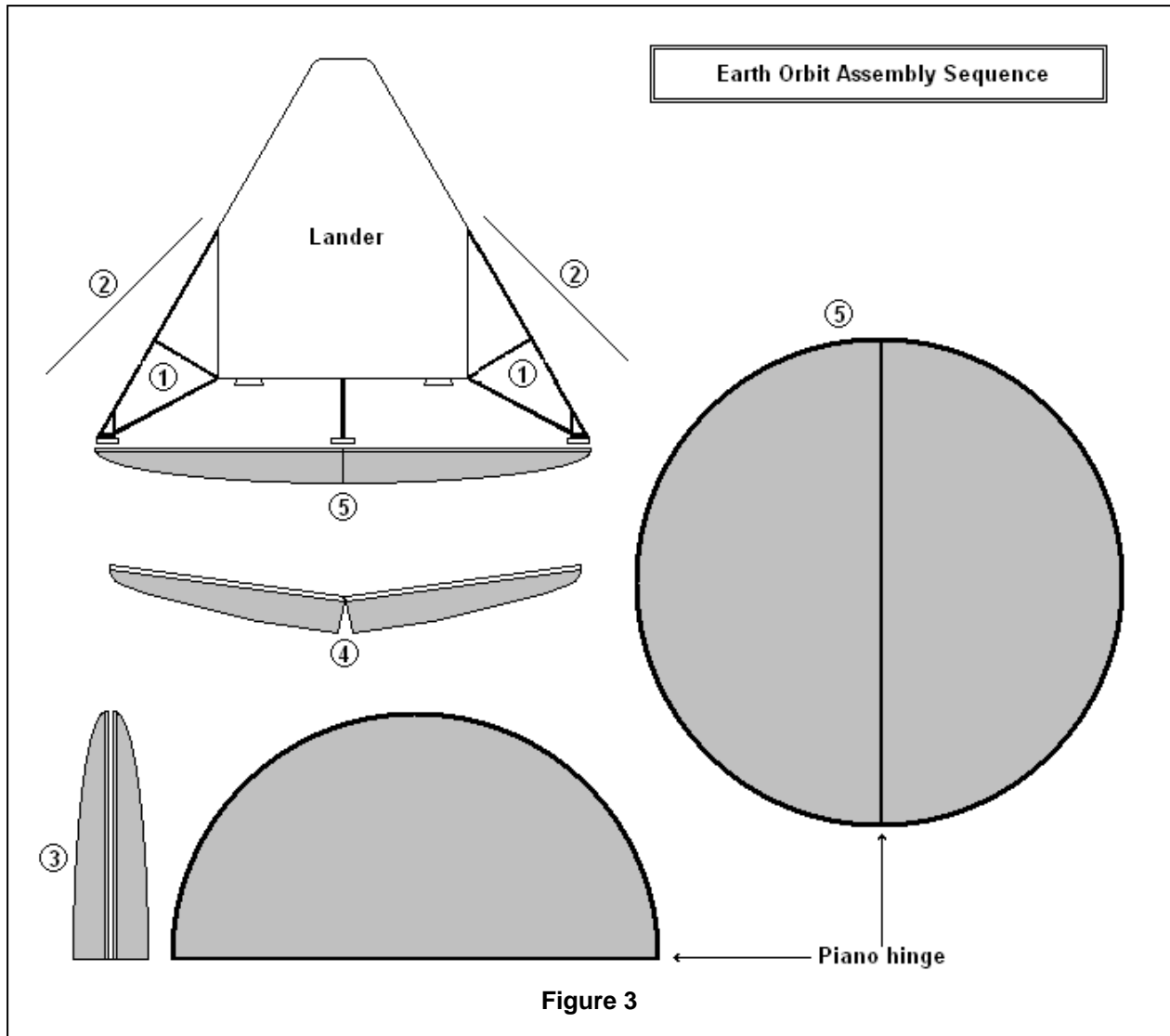
III.1 – The MarsDrive Common Lander – Heatshield Design

The MarsDrive Common Lander proposes a new ballistic aerobraking design that stays within the proven Apollo-legacy geometry, allows a 14.5 meter diameter heatshield, and fits within the 7.5 meter diameter payload limit. The design is shown schematically in Figure 2.



The vehicle is supported by a four-leg landing gear, each leg consisting of a foot-pad and a conventional 5-element support structure – one upper strut, two lower struts, and two cross-braces to provide lateral rigidity. The landing gear is stowed for Earth launch, giving the lander a fairing diameter of 7.5 meters. The spread of the deployed landing gear is 14.5 meters.

The primary aerobraking device is a 14.5-meter diameter carbon-carbon heatshield backed by fiber-form insulation. The heatshield and its support structure rest against the four landing pads as shown in Figure 3.1. The lander essentially “sits” on the heatshield. Two center braces (items ‘C’) are provided to support the center of the heatshield. The heatshield is split diagonally and joined with a 14.5-meter long piano hinge, allowing the heatshield to fold in half, shown as item ‘3’ in Figure 3. The resulting folded heatshield will then fit inside a 7.5-meter diameter fairing for Earth launch.



The area between the heatshield and the conic section of the lander is covered by an aeroshell (labeled “Aeroshell Fairing” in Figure 2 and item “2” in Figure 3), which provides protection during both aerocapture and aeroentry. The lander with the aeroshell in place presents a clean 30° truncated cone to the airstream leaving the heatshield.

Referring to Figure 3, after the Lander enters Low Earth Orbit, the landing gear (1) is deployed and locked in position. The aeroshell panels (2) are attached to the landing legs. The heatshield (3) is unfolded (4) into a complete disk (5) and attached to the landing pads and the center brace. During aerobraking, the windstream will compress the join where the heatshield folds, preventing plasma from encroaching into the join itself.

III.2 – Ejecting the Heatshield

The transition from aerobraking to powered flight begins as the lander approaches Mach 1. At this point the lander assumes a 0° angle of attack. The sequence is depicted in Figure 4.

1. The engines ignite. The ignition plume consumes 27 kg of propellant and produces 1,056 moles of exhaust gas. The sheltered space between the aft bulkhead, the heatshield, and the side-wall aeroshell is roughly 450 cubic meters. Using published NASA figures for their oxygen/methane CEV/SM engine [2], the combustion chamber pressure is 1,551 kPa (225 psia) and temperature is 3,500 Kelvin. Assuming an expansion ratio of 150:1 and adiabatic expansion of the exhaust gas, this should produce a pressure inside the closed shell of 10 kPa (1.5 psia).
2. As soon as engine ignition has been confirmed, the aeroshell panels are ejected. The engines come to full throttle.
3. The heatshield clamps are released and the heatshield retromotors (shown in Figure 2) are ignited. These four solid motors serve two purposes. They begin to drive the heatshield away from the lander and they cause the heatshield to begin to fold along the piano hinge.

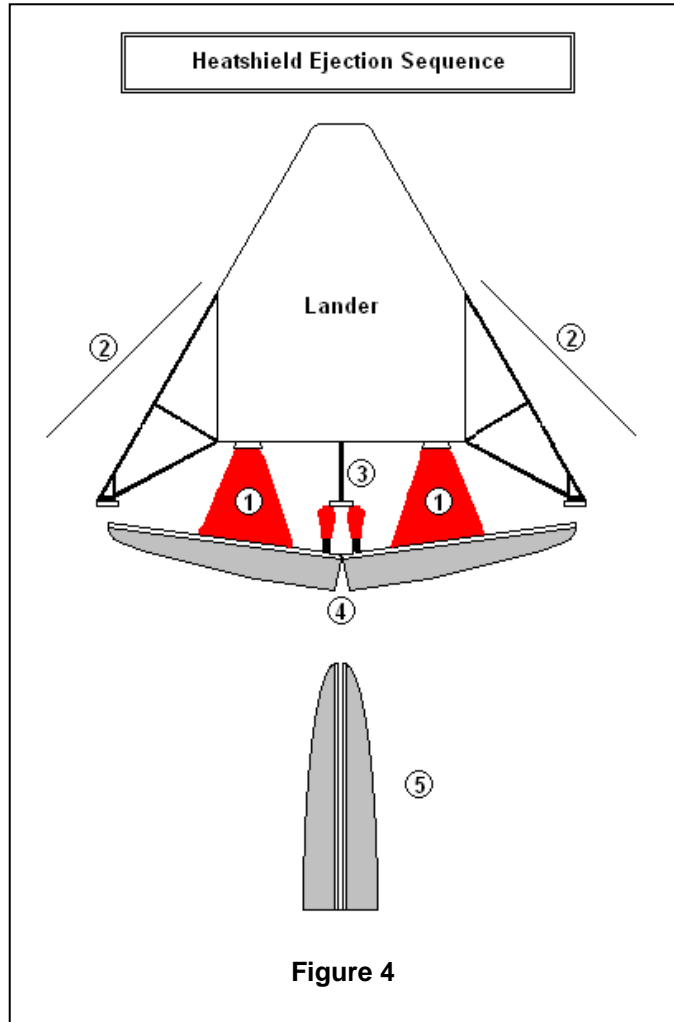


Figure 4

4. The hinged heatshield is in a state of unstable equilibrium. Once it begins to fold, airstream pressure will force the outer edges inward, continuing the folding.
5. The heatshield quickly folds into its collapsed state. This dramatically lowers the drag on the heatshield, which causes it to fall away from the decelerating lander.

Under full power the lander decelerates to a hover in 20 seconds. It then has approximately 300 seconds of propellant remaining to maneuver to its landing site under reduced power.

III.3 – The Common Lander Structure

The Common Lander is a truncated 30° conic section sitting on a 7.5 meter diameter cylindrical section. The total volume of both sections is 251 m³, not all of which is pressurized. The lander's pressure vessel structure is an aluminum honeycomb sandwich using Al 2024 for the face sheets and Al 5052 for the honeycomb core [4]. The pressure vessel structure mass was designed to withstand 9.5 psia nominal internal pressure. The assumed density for such a pressure vessel is 14 kg/m³. Key elements of the common lander geometry are given in Table 1.

The primary aerobraking device is a 14.5-meter diameter carbon-carbon heatshield backed by fiber-form insulation. The aerodynamic area of the heatshield is 165 m². Because carbon-carbon experiences no recession over the temperatures experienced during Mars aerocapture and aeroentry [3], only 1 mm of carbon-carbon is required. The fiber-form backing was sized at 10 cm to limit the bondline temperature to 250° C. The heatshield plus its support structure masses 4784 kg.

Lander Geometry (truncated cone over cylinder):	
Base Diameter:	7.5 m
Conic Angle:	30.0 deg
Diameter of truncation:	2.0 m
Height of truncated conic section:	4.76 m
Volume of truncated conic section:	93.8 m ³
Ground clearance:	2.5 m
Height of cylindrical section:	3.6 m
Volume of cylindrical section:	157.4 m ³
Total enclosed volume of lander:	251.2 m ³
Heatshield diameter:	14.5 m
Effective ballistic area:	165.1 m ²
Aeroshell surface area:	241.9 m ²

Table 1

The conic section of the lander and the area between the heatshield and the conic section of the lander is covered by an aeroshell which provides protection during both aerocapture and aeroentry. This aeroshell is composed of LI-2200, LI-900, Advanced Flexible Reusable Surface Insulation (AFRSI), and Flexible Reusable Surface Insulation (FRSI) at equal thicknesses over a support structure of graphite epoxy/Bismaleimide (BMI) composite skin panels. The aeroshell surface area, including the conical section of the common lander, is 242 m². The aeroshell masses 3677 kg.

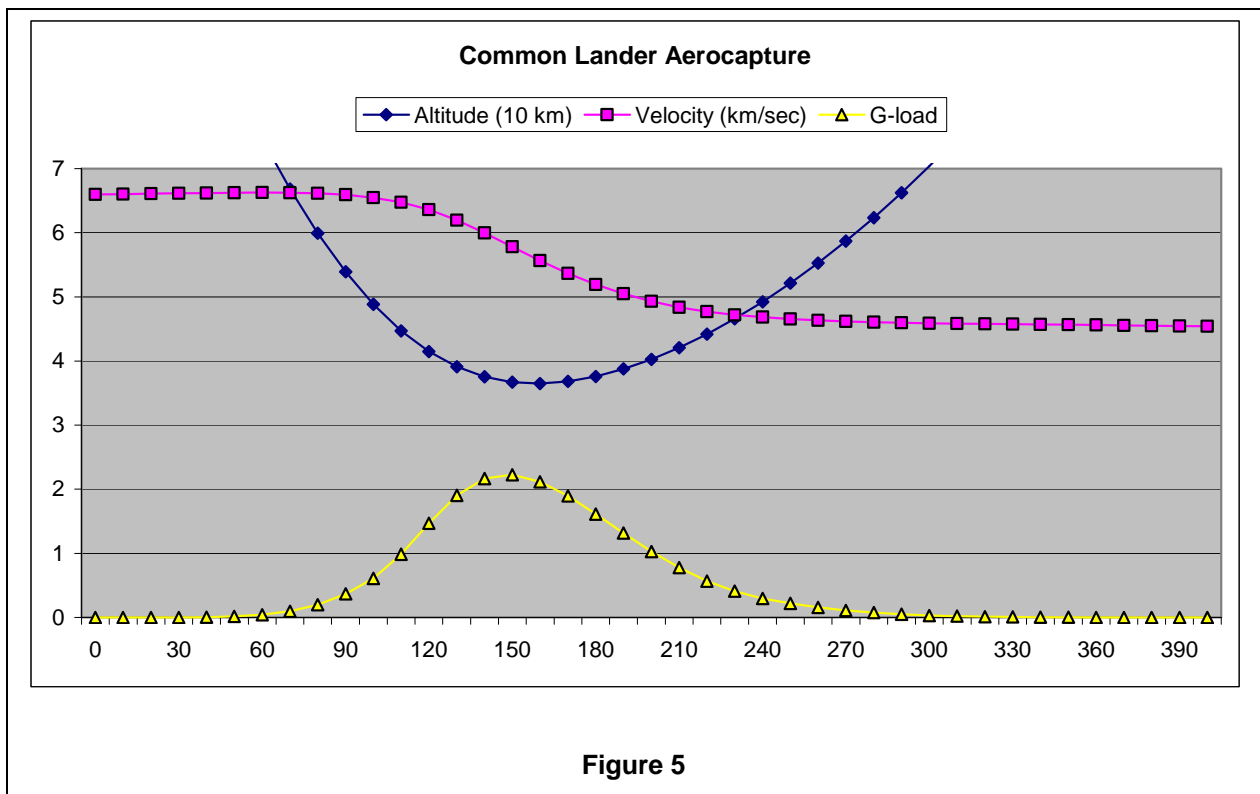
The Common Lander has one set of four engines and oxygen/methane propellant tankage which are used for descent and, in the case of the crewed lander, ascent. This gives the vehicle single-engine-out performance at all stages of both ascent and descent. As there is presently no engine that meets the Common Lander's requirements, design and development of this engine will be a major task facing MarsDrive. Place-holder dimensions and mass of this engine were patterned after the previously-published RL-60 oxygen/hydrogen engine specifications.

The engines are attached to the thrust structure at a point two meters above the bottom of the cylindrical section just above where the ascent stage separates from the landing deck on the crewed lander. The engine nozzles protrude through cut-outs in the lower 2 meters of the cylindrical section.

III.4 – Common Lander Aerocapture Simulation

In order to evaluate the Common Lander’s aerocapture, entry, descent, and landing characteristics, a simulation tool was developed to accurately predict the behavior of a spacecraft during entry into the Martian atmosphere (see Appendix I). This tool added an atmospheric model and lift/drag calculations to a pre-existing tool simulating spacecraft flight dynamics in the Sun-Earth-Mars gravitational environment.

The Lander aerocaptures into a highly-elliptical Mars orbit. Based on the simulated Earth-Mars transfer trajectory and a reasonable aerocapture alignment maneuver, aerocapture will place the lander and its service module in an orbit with an apoapsis of 3,171 km. An apoapsis ΔV of +30 m/s will raise the orbital periapsis to 181 km. The aerocapture pass is shown in Figure 5.



III.5 – Common Lander Aeroentry Simulation

The simulator was used to study the Lander’s aeroentry (EDL) profile. After the completion of orbital operations, the Lander deorbits by means of a 50 m/s ΔV burn. The ballistic aeroentry profile for a constant Lift/Drag ratio of 0.30 is shown in Figure 6. Active hypersonic entry guidance systems such as those being developed for near-future robotic missions [5] will allow the lander to fly a more optimal time-varying angle-of-attack profile. This should produce an improved entry profile.

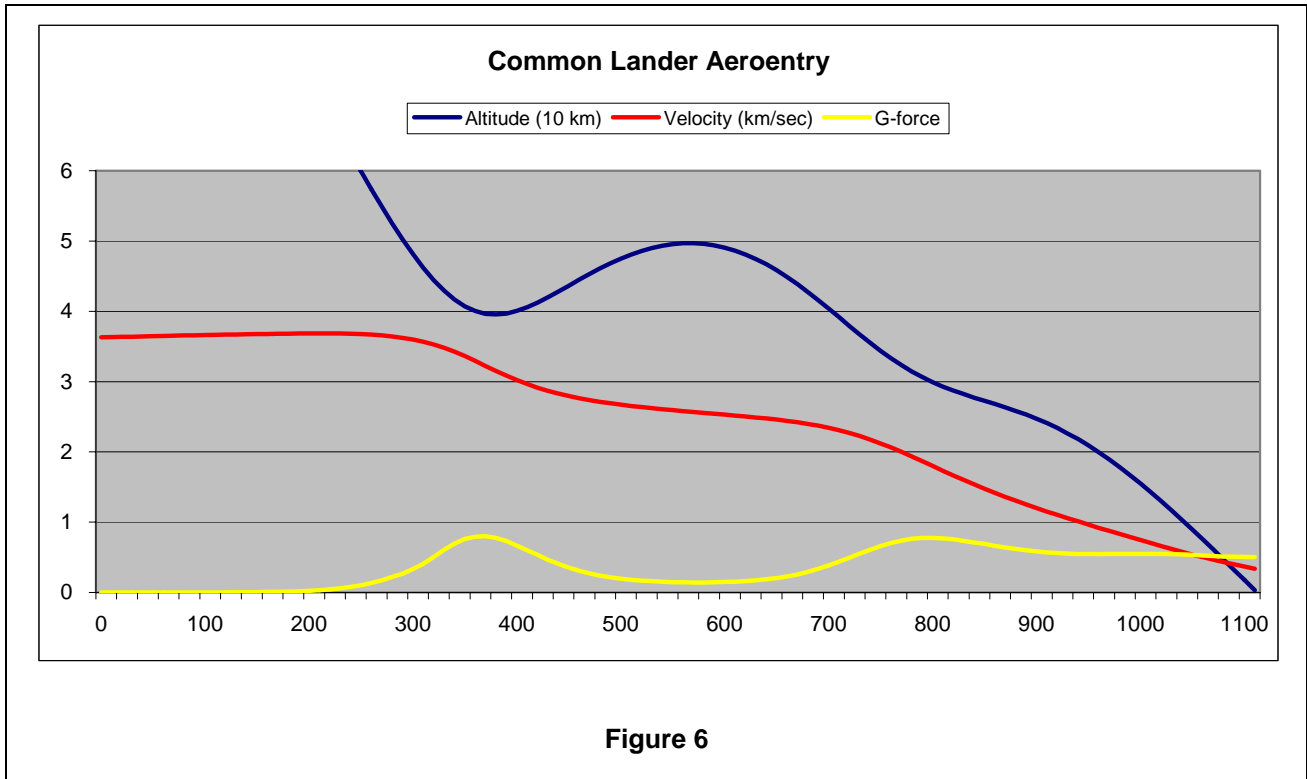


Figure 6

The lander will exit the plasma phase of its descent around 450 seconds after entry interface during the “roller-coaster” maneuver. At this point the landing zone beacons should be acquired, allowing the guidance computers to determine the optimal attitude to minimize the terminal cross-range maneuvering.

At 1100 seconds after entry interface, the lander has slowed to Mach 1.3 at 2 km MOLA. At this point the landing engines ignite and the heatshield is jettisoned as described earlier. Under full power the lander decelerates to a hover in 20 seconds at 0.5 km MOLA. It then has 300 seconds of propellant remaining to maneuver to the landing site and land.

IV – Conclusions

The MarsDrive Common Lander concept attempts to meet the requirements of landing crew and cargo vehicles on Mars of a mass sufficient to support a practical manned mission while meeting the launch vehicle parameters available in the foreseeable future. The concept attempts to minimize both risk and development cost by adhering to proven Apollo-legacy entry geometries.

The concept of the folding heatshield allows a practical heatshield to be carried within the 7.5 meter fairing limit assumed for near-term launch vehicles. The concept of igniting the landing engines in the sheltered space behind the heatshield avoids the very serious issue of igniting the engines in the face of a supersonic windstream.

MarsDrive is committed to developing technologies which will make human exploration of Mars practical. We believe this Common Lander concept is a step toward that greatest of all human adventures – the exploration and eventual colonization of the planet Mars.

Ronald M. Cordes
Director of Engineering
MarsDrive
rcordes@marsdrive.com
www.marsdrive.com

Appendix I

Simulating Aerocapture and Aeroentry

In order to evaluate the Common Lander's aerocapture, entry, descent, and landing characteristics, a simulation tool was developed to accurately predict the behavior of a spacecraft during entry into the Martian atmosphere. This tool added an atmospheric model and lift/drag calculations to a pre-existing tool simulating spacecraft flight dynamics in the Sun-Earth-Mars gravitational environment.

The NASA Mars Global Reference Atmospheric Model 2005 was used to create a mid-season, mid-latitude density profile of the Martian atmosphere below 140 km altitude. Inputting different seasonal and latitudinal data to Mars-GRAM-05 produce surprisingly different density profiles. One profile was chosen to produce a mid-season, low-latitude model which is representative of a reasonable entry profile. The atmospheric density model used is shown logarithmically in Figure I.1.

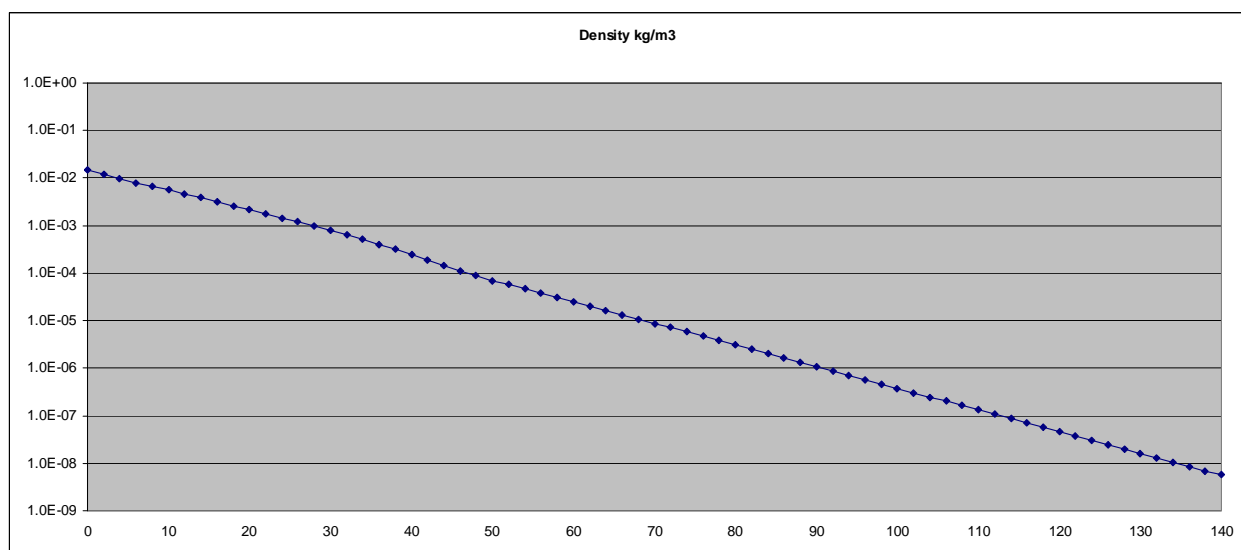


Figure I.1

Before any tool can be reliably used its results must be validated. For a simulator, the standard accepted validation methodology involves the simulation of one or more events whose outcome is already known, a process known as *Reconstruction Validation*.

The simulator was qualified by reconstructing the known entry profiles of three legacy Mars missions – Viking I, MER-A “Spirit” and Mars Pathfinder and one planned aerocapture mission – MSP-01.

Simulator Aerocapture Validation

Because there are no actual cases of successful aerocapture at Mars, this proved to be a challenge. As the best alternative available, we chose to reconstruct an aerocapture simulation done by simulation tools available within NASA.

In its initial design, the Mars Surveyor Program 2001 Orbiter (MSP-01) was to use aerocapture directly from its inbound transfer trajectory without a propulsive capture. This mission was studied carefully by NASA before being discarded in favor of a pure propulsive capture. Why this decision was made is speculative, but evidence points to a lack of faith in the then-existing Martian atmospheric models. Subsequent data obtained from various orbiting observers and from actual landed missions such as the two Mars Exploration Rovers have led to more reliable atmospheric models, culminating in the Mars-GRAM-05 model used herein. Table I.1 shows the physical parameters of the MSP-01 vehicle at Entry Interface.

MSP-01 Entry Interface Parameters	
Mass:	554 kg
Drag Coefficient:	1.68
Ballistic Area:	5.52 m ²
L/D Ratio (Up):	0.30
Entry Altitude:	140 km
Entry Velocity:	6600 m/s

Table I.1

This data was used as the initial conditions for the simulation, which was allowed to run for 300 seconds of mission time. Figure I.2 shows the comparison between the published MSP-01 altitude data and the data calculated by the simulator. In all figures, the MSP-01 data is in black with data points shown as black diamonds. The simulator output data is shown in red with square data points. The RMS of the difference between the two curves is 3.72 km.

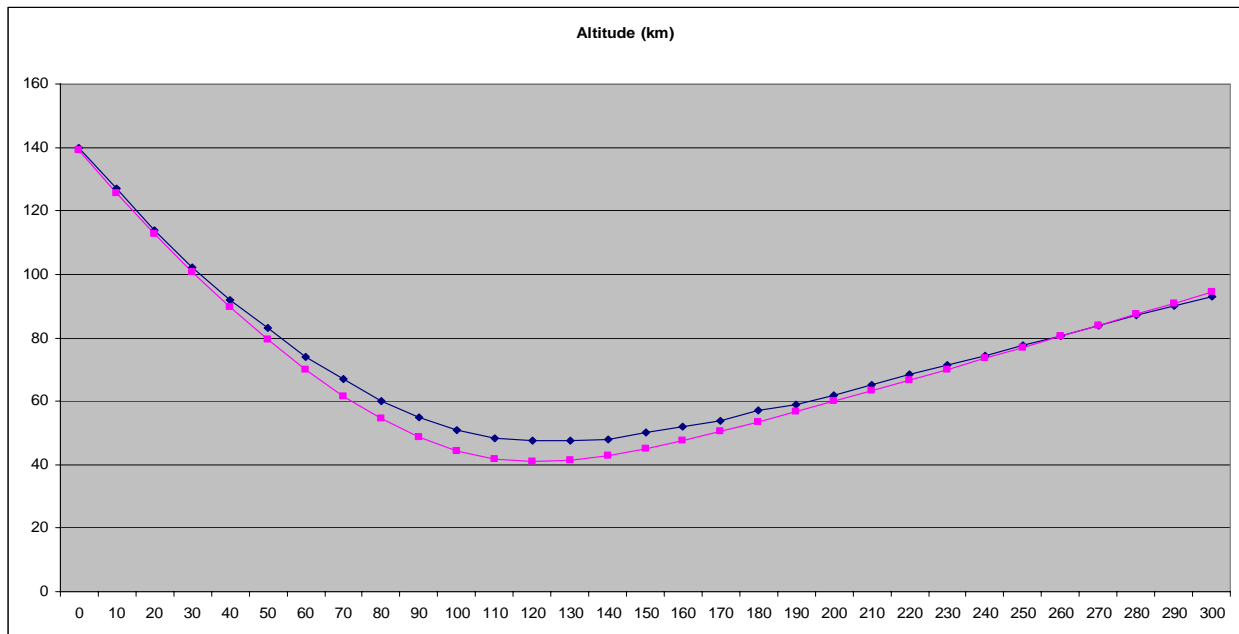


Figure I.2

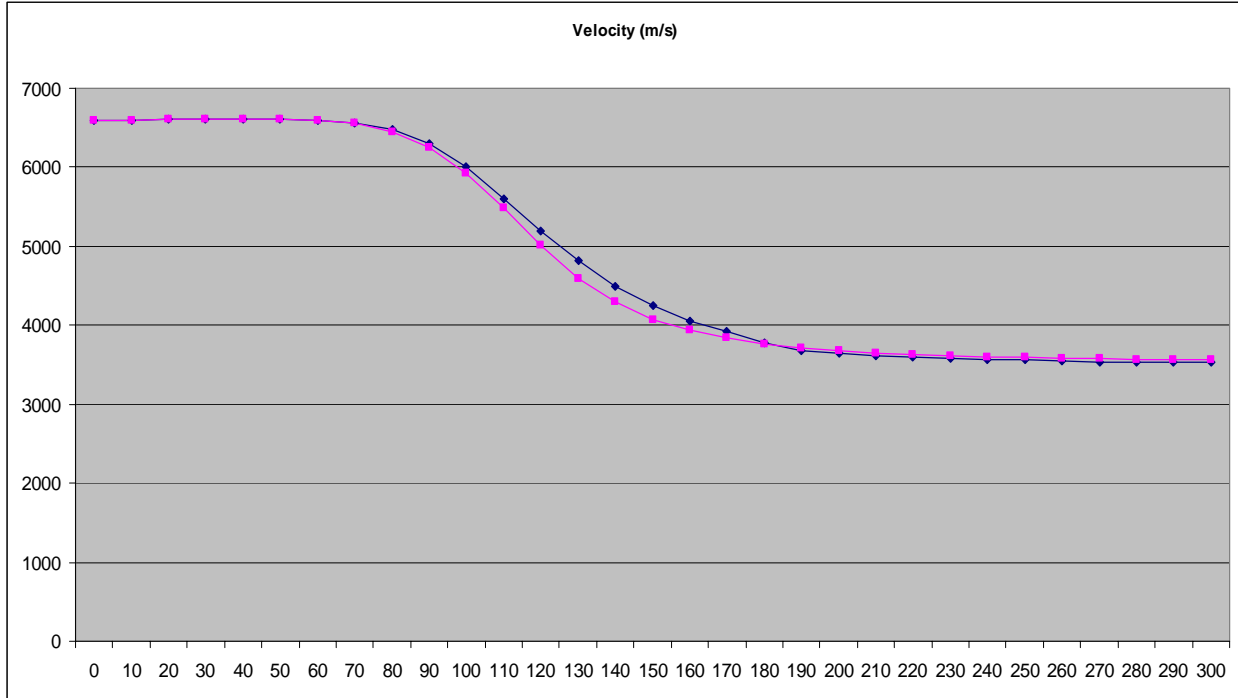


Figure I.3

Figure I.3 shows the comparison between the published MSP-01 velocity data and the data calculated by the simulator. The RMS of the difference between the two curves is 83.8 m/s.

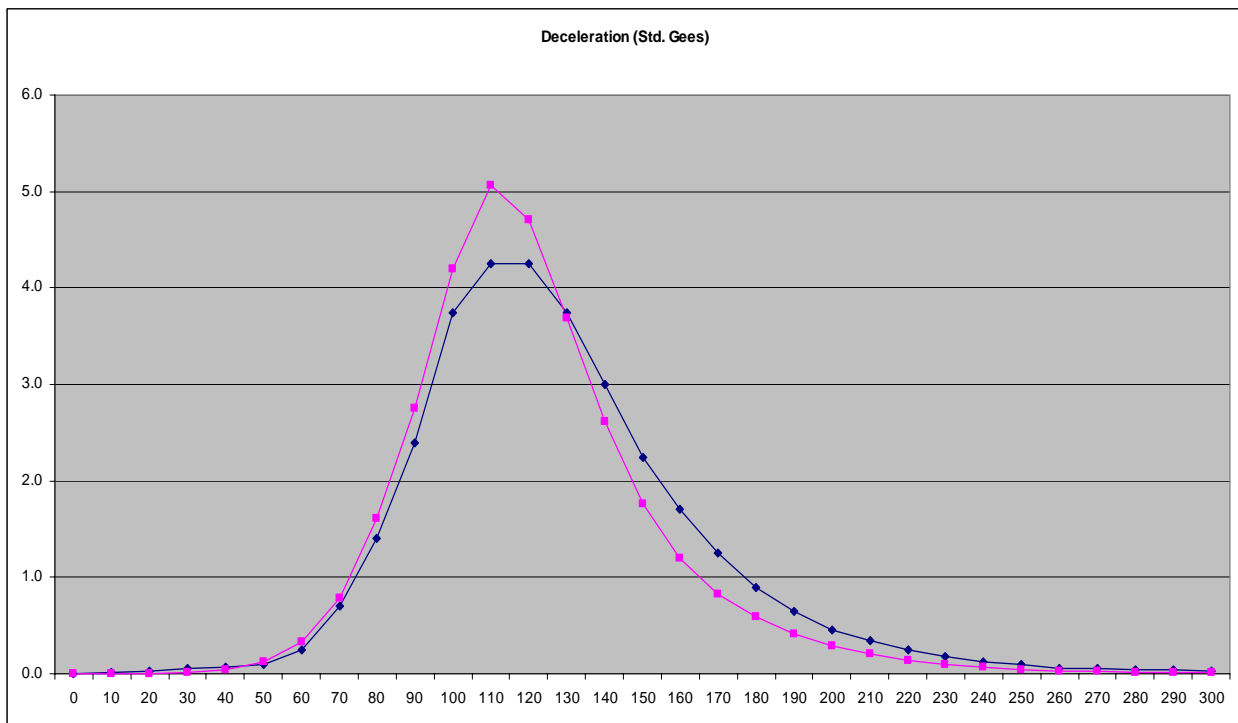


Figure I.4

Figure I.4 shows the comparison between the published MSP-01 deceleration data and the data calculated by the simulator. The RMS of the difference between the two curves is 0.273 g's.

It should be noted that in order to achieve the same exit altitude and velocity, the simulated spacecraft had to dive slightly deeper into the atmosphere than did the published MSP-01 vehicle. This discrepancy can be entirely explained by the differences in the atmospheric density models used by the original MSP-01 simulator and by this simulator. As the atmospheric model used by NASA in 1999 to obtain the published results is not available, this assumption is unproven, but seems entirely reasonable.

Simulator Aeroentry Validation

Braun and Manning [3] have compiled the physical and trajectory characteristics of five past successful Mars landings. We selected three very different legacy Mars missions – Viking I, MER-A “Spirit” and Mars Pathfinder to form the basis of our aeroentry reconstructions.

Braun and Manning do not publish the radial distance of the landers at their entry thresholds. Withers and Smith [6] do list the entry interface radial distances of MER-A and MER-B, but calculate entry velocities which are inconsistent with other published trajectory data for these missions. It was thus decided to use the Braun and Manning data and assume the entry altitude for all missions to be approximately 140 km, roughly the outer edges of the Martian atmosphere. As the velocity curves are relatively flat between 150 and 100 km altitude, this assumption does not materially affect the reconstruction results. It should also be noted that Withers and Smith report a large unknown in the angle of attack of the vehicles, which can lead to a significant variation in the parachute deployment data. Values within the given range of angles of attack were used by trial-and-error to obtain the best fit to the parachute deployment data for each mission.

Viking-1 Aeroentry Reconstruction

According to Braun and Manning, Viking-1 parachute deployment occurs at an altitude of 5.79 km and a velocity of Mach 1.1, corresponding to approximately 255 m/s. Angle-of-attack values were used by trial-and-error to obtain the best fit to the parachute deployment data. The results of the simulation are summarized in Table I.2.

The reconstructed altitude, velocity, and deceleration curves are shown in Figure I.5.

Viking-1 Aeroentry Reconstruction		
	Reported	Simulation
Mass at entry (kg):	992	992
Aerobrake diameter (m):	3.50	3.50
Ballistic Coefficient (kg/m ²):	64.0	64.0
Altitude at entry (km):	(see text)	139.5
Relative velocity at entry (m/s):	4700	4699
Flight path angle at entry (deg):	17.00	17.00
Angle of attack (deg):	11.00	12.72
Altitude at parachute deploy (km):	5.79	5.79
Relative velocity at parachute deploy (m/s):	255	255

Table I.2

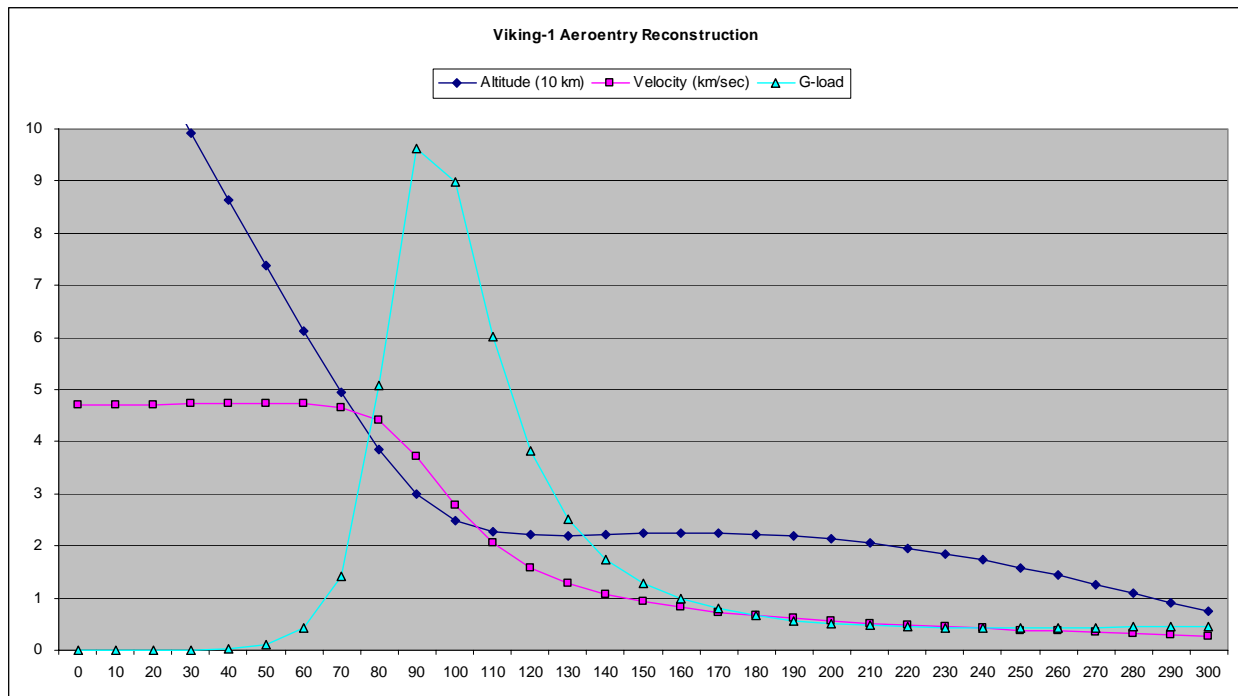


Figure I.5

MER-A “Spirit” Aeroentry Reconstruction

According to Braun and Manning, MER-A parachute deployment occurs at an altitude of 7.4 km and a velocity of Mach 1.77, corresponding to approximately 411 m/s. Angle-of-attack values were used by trial-and-error to obtain the best fit to the parachute deployment data. The results of the simulation are summarized in Table I.3.

The reconstructed altitude, velocity, and deceleration curves are shown in Figure I.6.

MER-A “Spirit” Aeroentry Reconstruction		
	Reported	Simulation
Mass at entry (kg):	827	827
Aerobrake diameter (m):	2.65	2.65
Ballistic Coefficient (kg/m ²):	94.00	94.01
Altitude at entry (km):	(see text)	139.89
Relative velocity at entry (m/s):	5400	5399
Flight path angle at entry (deg):	11.49	11.50
Angle of attack (deg):	0.0 ± 5.0	1.88
Altitude at parachute deploy (km):	7.40	7.40
Relative velocity at parachute deploy (m/s):	411	411

Table I.3

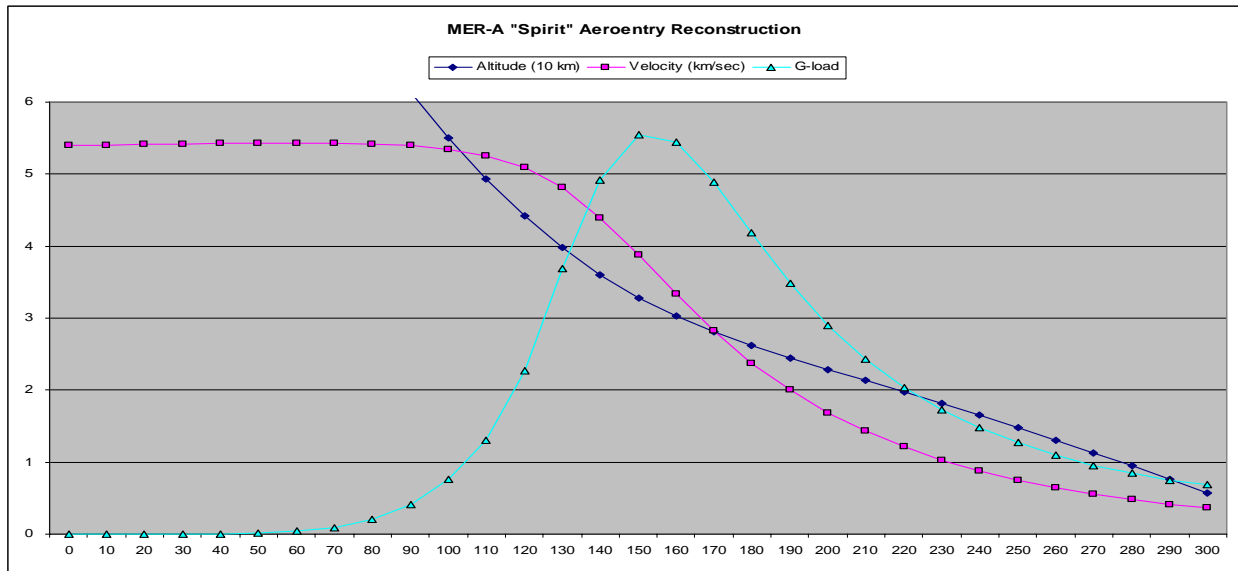


Figure I.6

Mars Pathfinder Aeroentry Reconstruction

According to Braun and Manning, MPF parachute deployment occurs at an altitude of 9.4 km and a velocity of Mach 1.57, corresponding to approximately 364 m/s. Angle-of-attack values were used by trial-and-error to obtain the best fit to the parachute deployment data. The results of the simulation are summarized in Table I.4.

The reconstructed altitude, velocity, and deceleration curves are shown in Figure I.7.

Mars Pathfinder Aeroentry Reconstruction		
	Reported	Simulation
Mass at entry (kg):	584	584
Aerobrake diameter (m):	2.65	2.65
Ballistic Coefficient (kg/m ²):	63.00	63.03
Altitude at entry (km):	(see text)	139.1
Relative velocity at entry (m/s):	7260	7258
Flight path angle at entry (deg):	14.06	14.00
Angle of attack (deg):	0.00	1.05
Altitude at parachute deploy (km):	9.40	9.40
Relative velocity at parachute deploy (m/s):	364	364

Table I.4

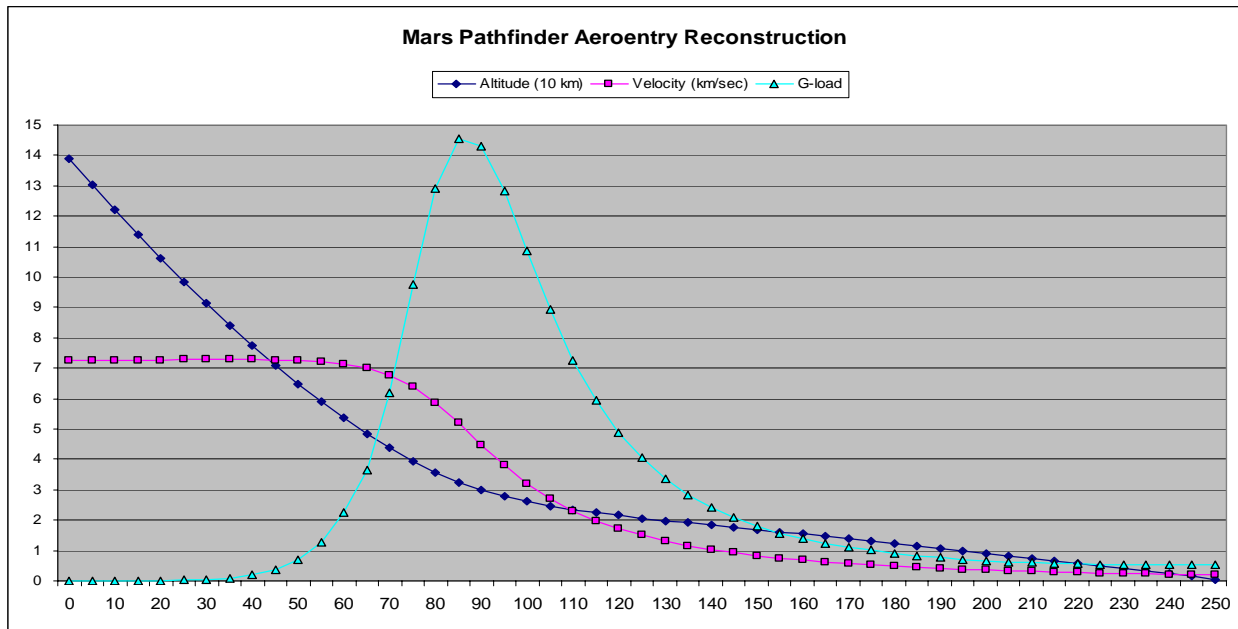


Figure I.7

References

- [1] “Sizing of an Entry, Descent and Landing System for Human Mars Exploration,” John A. Christian, Grant Wells, Jarret Lafleur, Kavya Manyapu, Amanda Verges, Charity Lewis and Robert D. Braun, Georgia Institute of Technology, preprint, 2006.
- [2] “NASA Exploration Systems Architecture Study”, NASA-TM-2005-214062.
- [3] “Mars Exploration Entry, Descent and Landing Challenges,” R.D. Braun and R.M. Manning, 2006 IEEE Aerospace Conference, March 2006.
- [4] Structural mass estimation data are from the NASA Exploration Systems Architecture Study, NASA-TM-2005-214062, November 2005.
- [5] “Advanced Hypersonic Entry Guidance for Mars Pinpoint Landing,” K. D. Mease, J. A. Leavitt, J. Benito, S. Talole, A. Salama, G. Sohl, M. Ivanov, and L. Ling, NSTC-07-0023, 2007.
- [6] “Atmospheric Entry Profiles from the Mars Exploration Rovers Spirit and Opportunity,” Paul Withers & Michael D. Smith, Icarus 185 (2006) 133-142.